JOURNAL OF ELECTROMAGNETIC ENGINEERING AND SCIENCE, VOL. 14, NO. 3, 278~283, SEP. 2014

http://dx.doi.org/10.5515/JKIEES.2014.14.3.278
ISSN 2234-8395 (Online) · ISSN 2234-8409 (Print)

Equivalent Model Analysis of Modified Satellite Antenna for Isoflux Pattern Generation

Eun-Cheol Choi · Jae Wook Lee* · Taek-Kyung Lee · Woo-Kyung Lee

Abstract

This paper presents a theoretical approach for a modified turnstile antenna suitable for satellite communication in order to investigate the current distributions of radiators and radiation characteristics with equivalent model analysis. The proposed equivalent model is composed of an ideally horizontal dipole antenna and vertically loaded top-hat radiating elements. The required isoflux pattern with wide beamwidth has been achieved by attaching top-hat elements to the main radiators. In addition to illustrating radiation patterns, electrical performances like current distributions have been analyzed by mathematically manipulating the equations derived from the equivalent horizontal and vertical dipole model.

Key Words: Circular Polarization (CP), Dipole Antenna, Equivalent Model, Isoflux Pattern, Turnstile Antenna.

I. Introduction

In a satellite communication, S-band antenna with its functions of telemetry, tracking, and command (TT&C) is an essential and fundamental component in monitoring and controlling the normal operation of satellite [1].

In general, a relatively low gain and wide beamwidth are required because communication should be available, even in the situations of changing altitude. Researchers have suggested several candidates for TT&C satellite antennas, including the microstrip patch [2], quadrifilar helix [3], conical spiral [4], and turnstile antenna [5-8]. The turnstile antenna, in particular, has several advantages, such as low complexity, easy fabrication, and robust characteristics with wide beamwidth.

This paper introduces a theoretical approach with equivalent model horizontal and vertical dipole elements. We validate our analysis by conducting mathematical manipulations and full-EM simulations using far-field approximations and the commercially available software CST Microwave Studio (CST MWS; Computer Simulation Technology AG., Darmstadt, Germany). In Section II, the equivalent model of the proposed antenna is dealt with using real dipole and image sources. The analysis of current distributions verified the relationship between the bowtie-shaped dipole and the wired dipole. In addition, a mathematical analysis of the modified dipole antennas is used to predict the electrical performances of the proposed antenna and compared them with the measured data of the fabricated antenna. A brief conclusion is provided in Section III.

II. Equivalent Model of Radiators

1. The Proposed Structure

Fig. 1 shows the geometry of the previously proposed antenna with structural modification and an isoflux pattern of circular polarization. As shown in Fig. 1, the radiators are composed of top-hat loaded bowtie-shaped dipole antennas with two feeding structures. Circular polarization with a wide beamwidth is generated by launching a Wilkinson power divider, which has a 90° phase difference and wide impedance bandwidth, below the ground plane.

The vertical top-hat elements have been attached specifically to

Manuscript received May 6, 2014 ; Revised August 11, 2014 ; Accepted August 12, 2014. (ID No. 20140506-020J)
School of Electronics, Telecommunication and Computer Engineering, Korea Aerospace University, Goyang, Korea.
*Corresponding Author: Jae Wook Lee (e-mail: jwlee1@kau.ac.kr)

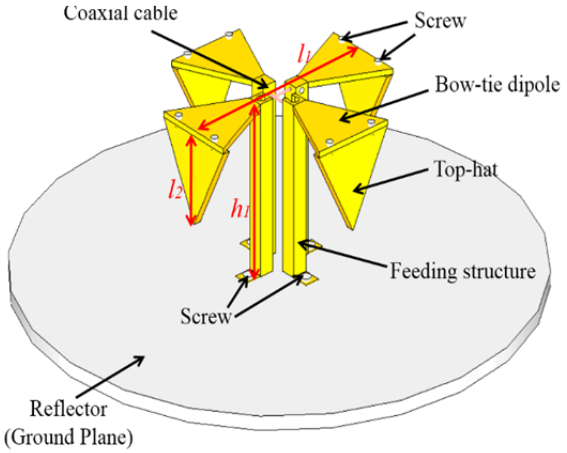

Fig. 1. The radiator part of *S*-band turnstile antenna [8].

generate a radiation pattern in a direction close to the ground plane. As a candidate receiving antenna working for a TT&C satellite, it covers the frequency range from 2,025 to 2,125 MHz in the satellite communication system. The important aspects for the proposed antenna are the enhancement of the axial ratio beamwidth affected by the vertically installed top-hat elements and beamwidth expansion of the isoflux pattern.

2. Equivalent Model of Top-Hat Loaded Antenna

For the mathematical evaluations of E-field distributions and to simplify the understanding of the radiation mechanism of the proposed antenna, the bowtie-shaped dipole elements is defined and modeled as simplified crossed dipole elements.

Fig. 2 shows the equivalent model of the proposed and modified turnstile dipole radiating elements by assuming the infinite ground plane of $\sigma = \infty$ and finite height of h_1. The entire structure of the radiators consists of the horizontal dipole and vertically loaded top-hat elements. The parameters l_1 and l_2 mean the lengths of horizontal dipole and vertical top-hat elements, respectively. In addition, θ and ψ are the angles from z-axis and y-axis to the observation point r, respectively.

The current distributions on the real source dipole elements can be approximated for the evaluation of the far-field radiation patterns as following equations [9].

$$I = \begin{cases} \hat{a}_y I_0 \sin[k(\frac{l_1}{2} + y')], \ (-\frac{l_1}{2} \le y' \le 0, \ z = h_1) \\ \hat{a}_y I_0 \sin[k(\frac{l_1}{2} - y')], \ (0 \le y' \le \frac{l_1}{2}, \ z = h_1) \end{cases} \quad (1)$$

$$I = \begin{cases} \hat{a}_z - I_0 \sin[k(-h_2 + z')], (h_2 \le z' \le h_1, \mathrm{y} = -\frac{l_1}{2}) \\ \hat{a}_z I_0 \sin[k(-h_2 + z')], (h_2 \le z' \le h_1, \mathrm{y} = \frac{l_1}{2}) \end{cases} \quad (2)$$

I_0 and k mean the maximum current value and the wavenumber,

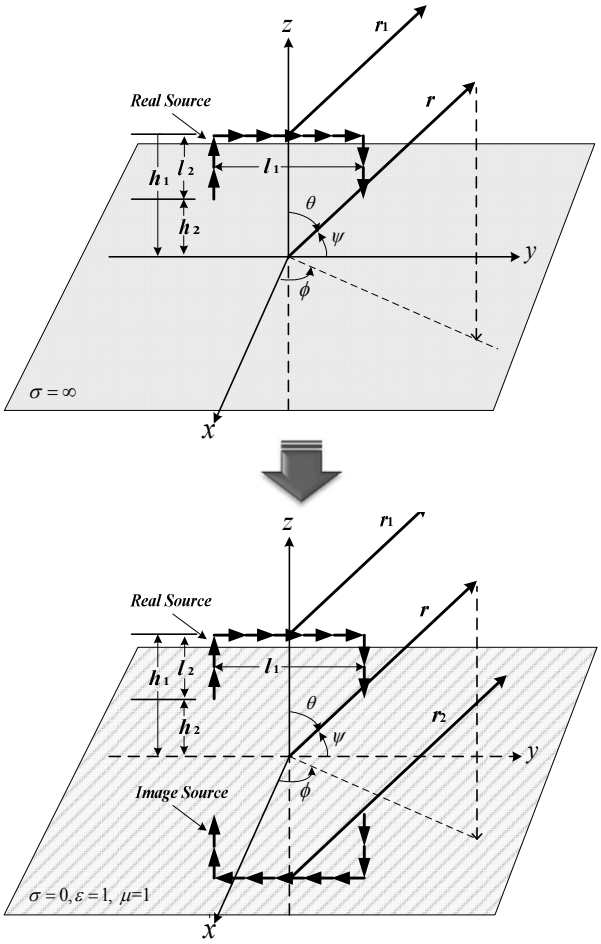

Fig. 2. Equivalent sources of horizontal dipole with top-hat elements.

respectively. Fig. 3 shows the surface current distributions on the bowtie-shaped dipole with top-hat elements and ideal dipole with vertical elements using the commercially available software CST MWS based on the finite-difference time-domain (FDTD) algorithm.

Fig. 3(a) shows the surface current distributions of the bowtie-shaped dipole which is a radiator in the designed turnstile antenna. As shown in Fig. 3(a), the vector current flow (real lines) can be divided into two basis components (dashed lines) relative to the main horizontal axis of bowtie radiator. The two opposite directions may cancel each other, while the other components remain and may be added positively. Consequently, the effect of actual current distribution will approach that of the ideal dipole antennas shown in Fig. 3(b).

For the validation of the assumed current distributions, the normalized current distributions obtained from mathematical representations in this work and CST MWS have been compared in Fig. 4 and show good agreement with a small discrepancy. As shown in Fig. 4, some discrepancies are evident in the results at dipole lengths of less than 30 mm, around 70 mm, and more than 110 mm. It can be expected that the reason is due to the feeding point for horizontal dipole and discontinuities in the connections between

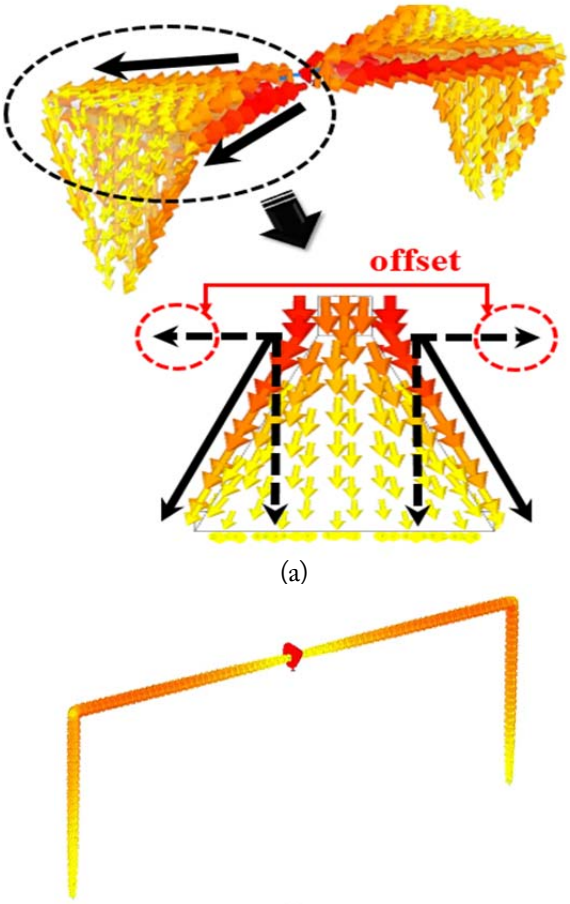

Fig. 3. The current distributions on the top-hat radiating elements. (a) Bowtie-shaped dipole and (b) ideal dipole with vertical elements.

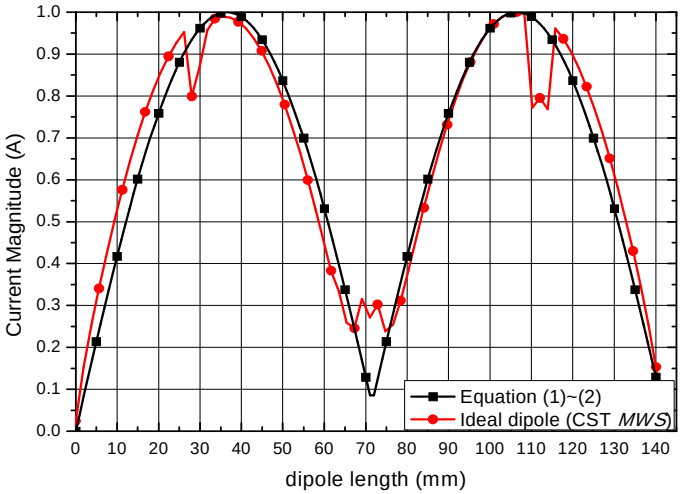

Fig. 4. The magnitude of normalized current on the horizontal dipole elements with top-hat loaded radiators.

vertical and horizontal elements. However, all three results using mathematical representations and CST simulation for two kinds of dipoles are nearly the same.

First of all, all the current distributions on the radiating elements without/with top-hat elements are assumed to be sinusoidal. The total radiated electric field can be obtained from the six components consisting of real source and image source effects (see Appendix).

Eqs. (3) and (4) show the far-zone radiated field of horizontal dipoles without/with top-hat elements, respectively.

$$E = -\frac{\eta I_0 k e^{-jkr}}{\pi r k \cos^2\theta}\sin(kh_1\cos\theta)\sin\psi \times \{\cos(\frac{kl_1\sin\theta}{2}) - \cos(\frac{kl_1}{2})\} \tag{3}$$

$$E = \frac{\eta I_0 e^{-jkr}\sin(k\frac{l_1}{2}\sin\theta)}{\pi r\sin\theta}[\cos(h_1 k\cos\theta)\cos(k(h_1-h_2) - \cos(h_2 k\cos\theta) + \sin(h_1 k\cos\theta)\sin(k(h_1-h_2)\cos\theta] + \frac{\eta I_0 e^{-jkr}\sin(kh_1\cos\theta)}{\pi r\cos\theta}[\cos(\frac{kl}{2}) - \cos(kl_2)\cos(\frac{kl_1\sin\theta}{2}) + \sin(kl_2)\sin(\frac{kl_1\sin\theta}{2})\sin\theta] \tag{4}$$

Fig. 5 shows the normalized radiation pattern when an ideal dipole without/with top-hat loaded elements are considered. As predicted from Fig. 5(a) and (b), the entire radiation pattern becomes broader, which means that radiation in the direction of 90° can be generated as the additionally vertical elements is attached. Hence, the enhancement of beamwidth can be accomplished because of the effects of the attached vertical dipoles.

In order to analytically investigate the change of the radiation pattern according to the length of top-hat loaded radiating elements and isoflux radiation pattern for covering all the target area uniformly, the proposed antenna is assumed to be installed on the PEC ground with an ideally infinite area. As shown in Fig. 6, it can be estimated from the mathematical representations using equivalent model and commercially available software based on EM full simulation that the radiation pattern could be changed by adjusting the height and the length of the top-hat radiating elements.

Fig. 6(a) and (b) show that the usage of a quarter wavelength in the distance between the ground plane and horizontal dipole elements results in the pattern of broadside direction perpendicular to the horizontal dipole elements. However, as the height increases, the gain in the broadside direction parallel to $\theta = 0°$ decreases. For example, it can be seen that no radiation occurs in the broadside direction if the height approaches a half wavelength. In addition, Fig. 6(c) and (d) delineate the effects according to the variations of parameter l_2, which is the length of top-hat loaded vertical elements.

For the gain and axial ratios of the proposed and modified turnstile antenna, simulations and measurements were carried out with the parameter values of $h_1 = 61$ mm and $l_2 = 31$ mm to determine the gain and axial ratios of the proposed and modified turnstile antenna, as shown in Fig. 7. By considering the mathematically equivalent model analysis, it can be ensured that the effect of the antenna height,

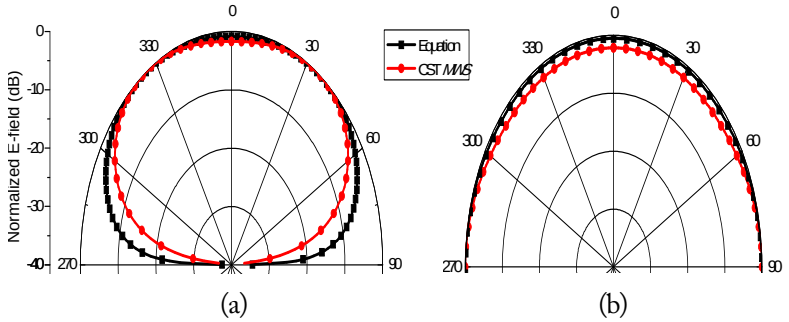

Fig. 5. The radiation pattern of dipole elements: (a) dipole without vertically loaded top-hat elements and (b) dipole with vertically loaded top-hat elements.

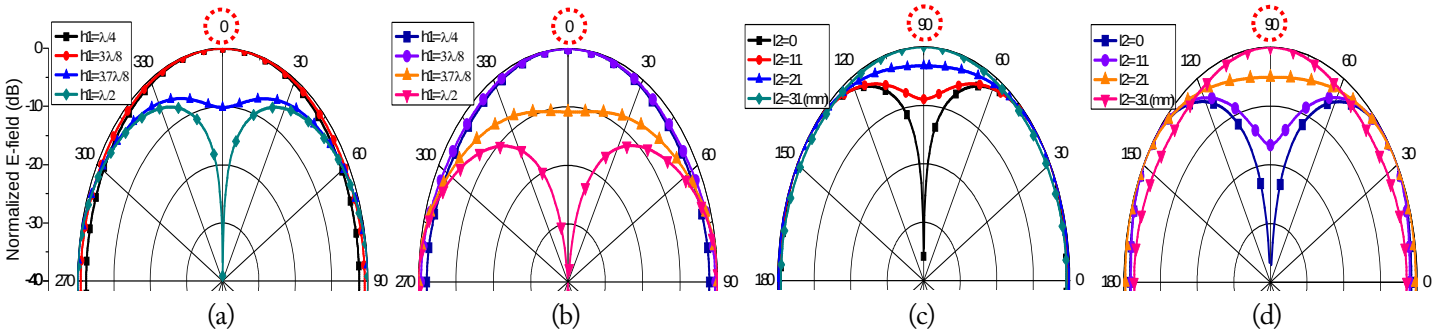

Fig. 6. The predicted radiation pattern using equivalent model of top-hat loaded antenna. (a) Mathematical results according to the variation of height h_1 when $l_2 = 31$ mm, (b) simulation results according to the variation of height h_1 when $l_2 = 31$ mm, (c) mathematical results according to the variation of length l_2 when $h_1 = 61$ mm, and (d) simulation results according to the variation of length l_2 when $h_1 = 61$ mm.

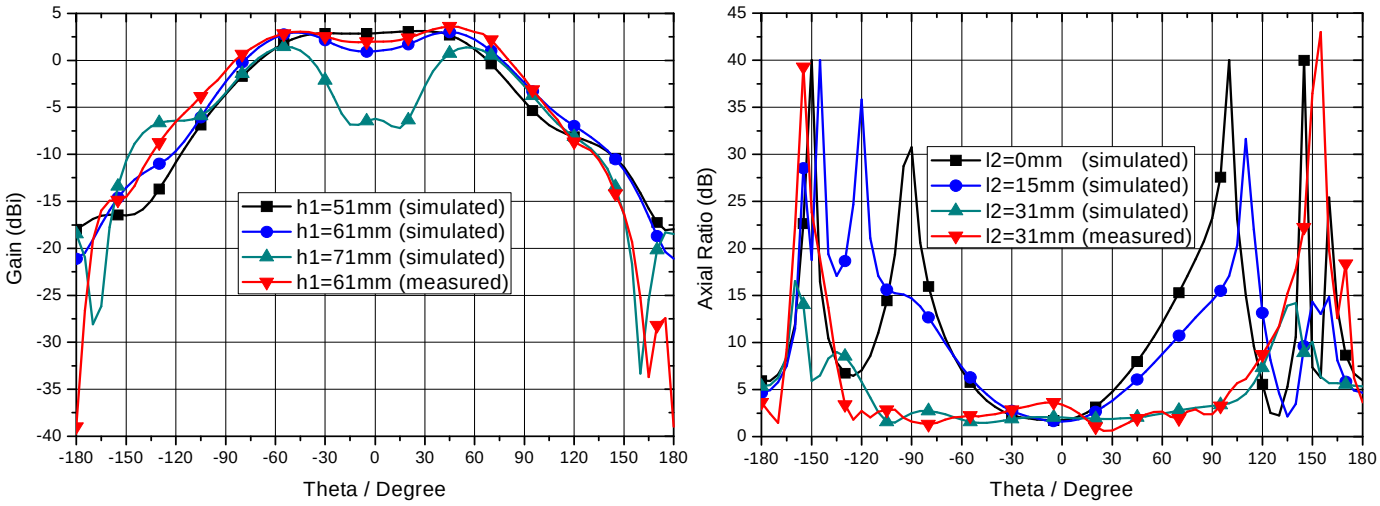

Fig. 7. Gain and axial ratio of the proposed antenna according to variation of h_1 and l_2 at f= 2,075 MHz: (a) right hand circular polarization (RHCP) gain and (b) axial ratios.

h_1, and the length of top-hat radiating element, l_2, on the radiation pattern and axial ratio is remarkably important relative to the other parameters.

III. Conclusion

An equivalent model of a top-hat loaded turnstile antenna has been developed by applying an image method and investigating current distributions on the radiating elements. The ideal dipole antennas and the proposed antenna were compared using the radiation pattern. A wide AR beamwidth was achieved with an isoflux pattern. It is ensured that the proposed equivalent model analysis can be effective for rapid design in terms of the radiation pattern and axial ratio in satellite communication.

Appendix

As shown in Fig. 2, the total radiation field can be estimated as a

sum of the radiated electric fields from the realized dipole sources and the imaged dipole elements. The differential electric field can be written as follows, by integration of the current distributions [9].

$$dE_\theta = j\eta \frac{kI_e(x',y',z')e^{-jkR}}{4\pi r} \times [\sin\theta \ or \ \sin\psi] \times [dz' \ or \ dy'], (dE_r = dE_\phi = 0) \tag{5}$$

$$E = \frac{j\eta k}{4\pi r} (\sin\theta \ or \ \sin\psi) \int_{-l/2}^{l/2} I_e(x',y',z')e^{-jkR} \times [dz' \ or \ dy'] \tag{6}$$

where I_e means the sinusoidal current on the dipoles. The phase variations for the observation points r_1 and r_2 can be expressed by assuming far-field conditions.

$$r_1 = r - h_1\cos\theta - y'\cos\psi, (\cos\psi = \hat{a}_y \cdot \hat{a}_r = \sin\theta\sin\phi) \tag{7}$$

and

$$r_2 = r + h_1\cos\theta - y'\cos\psi \tag{8}$$

Each electric field generated by real and image dipole sources reduces to

$$E = \frac{j\eta I_0 k e^{-jk(r-h_1\cos\theta)}}{4\pi r}\sin\psi[\int_{-\frac{l_1}{2}}^{0}\sin[k(\frac{l_1}{2}+y')]e^{jky'\cos\psi}dy' + \int_{0}^{\frac{l_1}{2}}\sin[k(\frac{l_1}{2}-y')]e^{jky'\cos\psi}dy'] \tag{9}$$

$$E = \frac{j\eta I_0 k e^{-jk(r+h_1\cos\theta)}}{-4\pi r}\sin\psi[\int_{-\frac{l_1}{2}}^{0}\sin[k(\frac{l_1}{2}+y')]e^{jky'\cos\psi}dy' + \int_{0}^{\frac{l_1}{2}}\sin[k(\frac{l_1}{2}-y')]e^{jky'\cos\psi}dy'] \tag{10}$$

It is apparent from (3) that the far-zone total electric field of horizontal dipoles without top-hat elements is equal to the sum of the fields (9) and (10).

In addition, the far-zone total electric field of horizontal dipoles with top-hat elements can be approximated as

$$E = \frac{j\eta I_0 k e^{-jk(r+\frac{l_1}{2}\cos\psi)}}{-4\pi r}\sin\theta\int_{h_2}^{h_1}\sin[k(-h_2+z')]e^{jkz\cos\theta}dz' \tag{11}$$

$$E = \frac{j\eta I_0 k e^{-jk(r+h_1\cos\theta)}}{4\pi r}\sin\psi[\int_{-\frac{l_1}{2}}^{0}\sin[k(\frac{l}{2}+y')]e^{jky'\cos\psi}dy' + \int_{0}^{\frac{l_1}{2}}\sin[k(\frac{l}{2}-y')]e^{jky'\cos\psi}dy'] \tag{12}$$

$$E = \frac{j\eta I_0 k e^{-jk(r-\frac{l_1}{2}\cos\psi)}}{4\pi r}\sin\theta\int_{h_2}^{h_1}\sin[k(-h_2+z')]e^{jkz\cos\theta}dz' \tag{13}$$

$$E = \frac{j\eta I_0 k e^{-jk(r+\frac{l_1}{2}\cos\psi)}}{-4\pi r}\sin\theta\int_{-h_1}^{-h_2}\sin[k(-h_2-z')]e^{jkz\cos\theta}dz' \tag{14}$$

$$E = \frac{j\eta I_0 k e^{-jk(r+h_1\cos\theta)}}{-4\pi r}\sin\psi[\int_{-\frac{l_1}{2}}^{0}\sin[k(\frac{l}{2}+y')]e^{jky'\cos\psi}dy' + \int_{0}^{\frac{l_1}{2}}\sin[k(\frac{l}{2}-y')]e^{jky'\cos\psi}dy'] \tag{15}$$

$$E = \frac{j\eta I_0 k e^{-jk(r-\frac{l_1}{2}\cos\psi)}}{4\pi r}\sin\theta\int_{-h_1}^{-h_2}\sin[k(-h_2-z')]e^{jkz\cos\theta}dz' \tag{16}$$

The total electric field is the sum of fields from (11) to (16), where Eqs. (11)–(13) are caused by the real source located above the ground and Eqs. (14)–(16) are from the image source.

This research was supported by the National Space Lab (NSL) program through the Korea Science and Engineering Foundation funded by the Ministry of Education, Science and Technology (No. S10801000159-08A0100-15910).

REFERENCES

[1] Y. G. Jang, and D. H. Lee, *Satellite System Design Engineering*. Seoul, Korea: KyungMoon Publishers, 1997.

[2] A. M. El-Tager, M. A. Eleiwa, and M. I. Salama, "A circularly polarized dual-frequency square patch antenna for TT&C satellite applications," in *Proceedings of Progress in Electromagnetics Research Symposium (PIERS)*, Beijing, China, 2009, pp. 23−27.

[3] I. Gonzalez, J. Gomez, A. Tayebi, and F. Catedra, "Optimization of a dual-band helical antenna for TTC applications at S band," *IEEE Antennas and Propagation Magazine,* vol. 54, no. 4, pp. 63−77, Aug. 2012.

[4] K. F. A. Hussein, "Conical linear spiral antenna for tracking, telemetry and command of low earth orbit satellites," *Progress in Electromagnetics Research C*, vol. 29, pp. 97−107, Apr. 2012.

[5] S. X. Ta, J. J. Han, I. Park, and R. W. Ziolkowski, "Wide-beam circularly polarized crossed scythe-shaped dipoles for global navigation satellite systems," *Journal of Electromagnetic Engineering and Science*, vol. 13, no. 4, pp. 224−232, Dec. 2013.

[6] K. J. Lee, D. J. Woo, T. K. Lee, and J. W. Lee, "Circularly polarized antenna with wide axial-ratio bandwidth," *Journal of Korean Institute of Electromagnetic Engineering Science*, vol. 21, no. 7, pp. 842−849, Jul. 2010.
[7] E. C. Choi, J. W. Lee, T. K. Lee, and W. K. Lee, "Circularly polarized S-band satellite antenna with parasitic elements and its arrays," *IEEE Antennas and Wireless Propagation Letters*, 2014, http://dx.doi.oirg/10.1109/LAWP.2014.2347998.
[8] E. C. Choi, J. W. Lee, and T. K. Lee, "Modified S-band satellite antenna with isoflux pattern and circularly polarized wide beamwidth," *IEEE Antennas and Wireless Propagation Letters*, vol. 12, pp. 1319−1322, Oct. 2013.
[9] C. A. Balanis, *Antenna Theory: Analysis and Design*, 3rd ed. Hoboken, NJ: Wiley, 2005.

Eun-Cheol Choi

received the B.S. and M.S degree in electronics, telecommunications, and computer engineering from Korea Aerospace University, Goyang, Korea, in 2012 and 2014, respectively. His research interests include satellite communication antenna design and analysis. His current interest is measurement of composite material.

Taek-Kyung Lee

received the B.S. degree in electronic engineering from Korea University, Seoul, Korea, in 1983, and the M.S. and Ph.D. degrees in electrical engineering from the Korea Advanced Institute of Science and Technology, Seoul, in 1985 and 1990, respectively. From May 1990 to April 1991, he was a Postdoctoral Fellow with the University of Texas at Austin (under a grant from the Korea Science and Engineering Foundation). From August 1991 to February 1992, he was with the Korea Advanced Institute of Science and Technology. In March 1992, he joined the faculty of Korea Aerospace University, Goyang, Korea, where he is currently a Professor with the School of Electronics, Telecommunication, and Computer Engineering. From July 2001 to July 2002, he was an Associate Visiting Research Professor with the University of Illinois at Urbana-Champaign. His research interests include computational electromagnetics, antennas, analysis and design of microwave passive circuits, and geophysical scattering.

Jae Wook Lee

received the B.S. degree in electronic engineering from Hanyang University, Seoul, Korea, and the M.S. and Ph.D. degrees in electrical engineering (with an emphasis in electromagnetics) from Korea Advanced Institute of Science and Technology (KAIST), Daejeon, Korea, in 1992, 1994, and 1998, respectively. From 1998 to 2004, he was a senior member in the Advanced Radio Technology Department, Radio and Broadcasting Research Laboratory, Electronics and Telecommunications Research Institute (ETRI), Daejeon. He later joined the School of Electronics, Telecommunications and Computer Engineering, Korea Aerospace University, Korea, where he is currently a Professor. His research interests include high power amplifier design, computational electromagnetics, EMI/EMC analysis on PCB, and component design in microwave and millimeterwave.

Woo-Kyung Lee

received the B.Sc. and M.Sc. degrees from the Korea Advanced Institute of Science and Technology (KAIST), Seoul, Korea, in 1990 and 1994, and the Ph.D. degree from the University College London, United Kingdom, in 2000, all in electrical engineering. From 1999 to 2002, he worked as a Research Professor at SaTReC, KAIST, and was involved in developing communication and antenna systems for small satellite systems. From 2003 to 2004, he worked at Samsung Advanced Institute of Technology for UWB, antenna, communication system researches. In 2004, he joined the Electrical Engineering and Avionics Department, Korea Aerospace University, Seoul, Korea, where he currently works as an Associate Professor. His research interests are in the area of communication and radar system design, spaceborne antenna development, image processing, and electronic counter measure and electronic counter counter measure techniques.